ChemComm

COMMUNICATION

View Article Online
View Journal | View Issue

Open Access Article. Published on 24 March 2022. Downloaded on 12/4/2025 8:37:25 AM.
This article is licensed under a Creative Commons Attribution 3.0 Unported Licence.

Check for updates

Cite this: *Chem. Commun.*, 2022, **58**, 4981

Received 24th February 2022,
Accepted 21st March 2022

DOI: 10.1039/d2cc01136k

rsc.li/chemcomm

A stereoselective hydride transfer reaction with contributions from attractive dispersion force control†

D. Christopher Braddock,* Natnicha Limpaitoon, Krzysztof Oliwa, Daniel O'Reilly, Henry S. Rzepa* and Andrew J. P. White

The experimentally determined stereochemical outcome of an unprecedented hydride transfer from a lithium alkoxide to an aldehyde is reported, as deconvoluted by the combined use of a single enantiomer alkoxide in conjunction with a deuterium label. The stereoselective outcome is consistent with a computationally predicted transition state model stabilised by contributions from attractive dispersion forces.

Recently, we reported the addition of the lithium acetylide of alkyne **1** to adamantane carboxaldehyde **2** unexpectedly produced quantities of ynone **3** and adamantane methanol **4** (Fig. 1).[1] We invoked a hydride transfer in a six-membered chair-like transition state (**TS A**) from the initially formed secondary lithium alkoxide AdCH(C≡C^{t}Bu)OLi to still unreacted AdCHO to explain this observation. In line with this explanation, isolation of the expected addition product **5**, and reformation of the lithium alkoxide in the presence of AdCHO **2** gave the same products.[1] While the transfer of hydride from LiCCH (*e.g.*, ^{t}BuLi)[2] and LiNCH (*e.g.*, LDA)[3] motifs to carbonyl compounds are well precedented, to the best of our knowledge the above example constitutes the only known example of hydride transfer from a LiOCH atomic tetrad to an aldehyde.[4] We had noted that this outcome could be linked to the particular structure of this secondary alkoxide whereby steric compression of the adamantyl bearing sp^3 centre is simultaneously relieved as the formation of conjugated ynone **3** acts as a thermodynamic driving force. While these two factors seem intuitive to the organic chemist, and where we invoked **TS A** with the adamantyl groups of both components in equatorial positions, herein we provide computational and experimental evidence for a third factor at work: attractive dispersion forces that help stabilise a transition state that we initially formulated with the adamantyl grouping of the aldehyde as occupying an axial position (**TS B**).

Prior to undertaking experimental studies, transition state computational modelling was undertaken. DFT procedures were based on the following four models: (i) Li coordination with 2 explicit thf solvent molecules; 2thf@B3LYP + GD3BJ/Def2-SVPP/SCRF = thf; (ii) 2thf@B3LYP + GD3BJ/Def2-TZVPP/SCRF = thf; (iii) model (i) with 3thf and; (iv) model (ii) with 3thf (Fig. 2, top).[5] These models are all consistent in predicting that using the lithium alkoxide of (*S*)-**5** results in a transition state for the (*S*,*Si*)-diastereoisomer (**TS B**) for which $\Delta G^{\ddagger}_{298}$ is ∼0.3–0.8 kcal mol^{-1} lower than the (*S*,*Re*)-transition state diastereoisomer (**TS A**) using the 2thf solvent model and ∼3 kcal mol^{-1} lower (∼3.3 kcal mol^{-1}@195K) using the 3thf solvent model;[6] the dispersion stabilisation contribution (B3LYP + GD3BJ) for this latter value is ∼1.2 kcal mol^{-1}, which suggests a significant contribution from dispersion effects. Non-covalent interaction (NCI) analysis[6] indicates this originates at least in part from the region where the alkynyl-*t*-butyl and adamantyl (from the aldehyde) groups are proximate and which are absent from **TS A** (Fig. 2, bottom). Further inspection of the calculated transition state geometry for **TS B** – originally formulated as a chair-like transition state (*c.f.* Fig. 1) – reveals instead that the

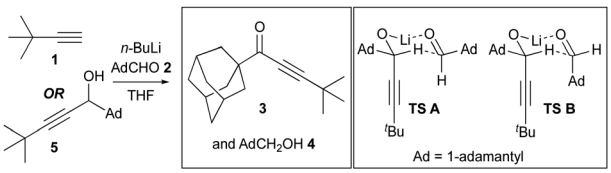

Fig. 1 Unexpected products of hydride transfer (boxed left). Transition states **A** and **B** (boxed right).

Department of Chemistry, Imperial College London, Molecular Sciences Research Hub, White City Campus, London W12 0BZ, UK.
E-mail: c.braddock@imperial.ac.uk, h.rzepa@imperial.ac.uk;
Tel: +44(0)2075945772

† Electronic supplementary information (ESI) available: Experimental procedures and characterising data; X-ray crystallographic details for **7**; copies of ^{1}H and ^{13}C NMR spectra; HPLC e.r. determinations; VCD spectrum for (*R*)-**4**-*d*. CCDC 2151865. For ESI and crystallographic data in CIF or other electronic format see DOI: 10.1039/d2cc01136k

Open Access Article. Published on 24 March 2022. Downloaded on 12/4/2025 8:37:25 AM.
This article is licensed under a Creative Commons Attribution 3.0 Unported Licence.

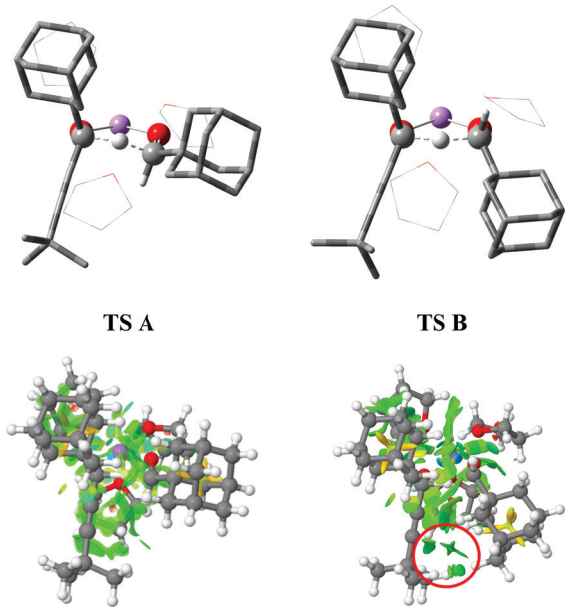

Fig. 2 (top) Calculated geometries of **TS A** and **TS B** with three explicit THF solvent molecules showing the distorted half-chair and coplanar nature of the six atoms of the cycles respectively; (bottom) NCI plots derived from the total electron density (B3LYP + GD3BJ/Def2-TZVP) for **TS A** and **TS B** showing the weakly attractive regions (green) between the alkynyl-*t*-butyl and adamantyl groups in **TS B** (red circle), which are not present in **TS A**. See reference 6 for a clickable link to interactive 3D transition state models and NCI isosurfaces.

six atoms of the cycle are essentially coplanar. For **TS A**, a distorted half-chair conformation is evident, but also with significant co-planarity in the ring. In these situations, axial and equatorial descriptors clearly do not apply.‡ Notwithstanding the conformations adopted by each of the two transition state geometries as revealed by computations, we sought to devise an experiment that could discriminate between them.

To investigate this experimentally we proposed that transition states **A** and **B** could be differentiated by judicious combined use of a single enantiomer alcohol and a deuterium label (Fig. 3). Thus, we envisaged tracking the stereochemical course of reaction of single enantiomer deuterated alcohol **5**-*d* (after deprotonation to the lithium alkoxide) with AdCHO **2** and/or the reaction of single enantiomer alcohol **5** (after deprotonation to the lithium alkoxide) with AdCDO **2**-*d*.

Accordingly, our studies commenced by the reduction of readily available adamantanecarboxyaldehyde **2**[1] with inexpensive sodium

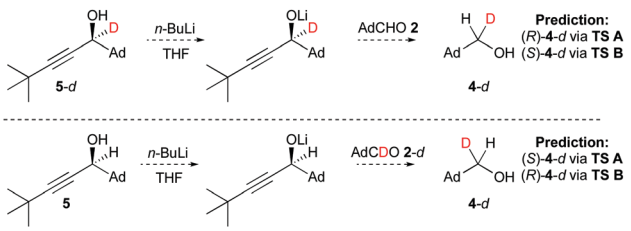

Fig. 3 Proposed combined single enantiomer-deuterium labelling experiments to differentiate transitions states **A** and **B**.

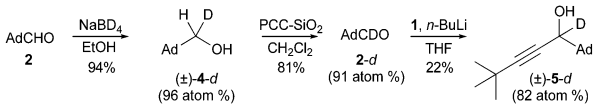

Scheme 1 Synthesis of labelled propargylic alcohol (±)-**5**-*d*.

borodeuteride to give monodeuterated alcohol (±)-**4**-*d* (Scheme 1).§ To our delight, simple reoxidation with pyridinium chlorochromate-silica[7] provided aldehyde **2**-*d* with high deuterium content evidently under the control of a primary kinetic isotope effect.[8] To the best of our knowledge this tactic has not previously been reported in the literature for the preparation of deuterated aldehydes and it is our expectation that this should prove to be a general approach.[9] Subsequent lithiation of terminal alkyne **1** and addition to aldehyde **2**-*d* under the conditions reported for the formation of (±)-**5**[1] gave novel propargylic alcohol (±)-**5**-*d*.¶

Prior to investing effort in enantiomeric resolution of secondary alcohol (±)-**5**-*d*, a preliminary attempted deuteride transfer by treating (±)-**5**-*d* with *n*-BuLi and AdCHO **2** (1 : 1 : 3, 0 °C to r.t., 16h), showed no evidence for the formation of alcohol (±)-**4**-*d* by deuteride transfer. Instead, *non*-deuterated alcohol **4** was observed as the major product in a complex mixture where all of aldehyde **2** had been consumed. We therefore invoke faster Tischenko-type hydride transfers (consuming the aldehyde) over the proposed and evidently KIE-retarded deuteride transfer.‖

Undaunted by the failure to transfer deuteride anion to AdCHO, attention turned to the other possible experiment, *viz.* transfer of hydride to AdCDO (*cf.*, Fig. 3). Accordingly, derivatisation of previously reported propargylic alcohol (±)-**5**[1] with (*S*)-camphanic acid chloride gave the expected 1 : 1 mixture of diastereomeric esters **6** and **7** in high yield, from which ester **7** could be obtained directly as a single diastereoisomer by fractional crystallisation (Scheme 2) as confirmed by X-ray crystallography (Fig. 4).** Ester hydrolysis gave single enantiomer propargylic alcohol (*S*)-**5**, as confirmed by HPLC studies of its benzoate ester on a chiral stationary phase by comparison to a racemic sample.**

Much to our delight, subsequent treatment of single enantiomer (*S*)-**5** with *n*-BuLi and AdCDO **2**-*d* allowed isolation of deuterated alcohol **4**-*d* (Scheme 3).†† Isolated alcohol **4**-*d* showed a small but negative optical rotation [−2.41, *c* 1.87, $CHCl_3$; −1.39 ± 0.55σ (16 measurements), *c* 1.08, cyclopentane] allowing assignment as enriched in the (*R*)-enantiomer by comparison with the previously reported positive rotation for

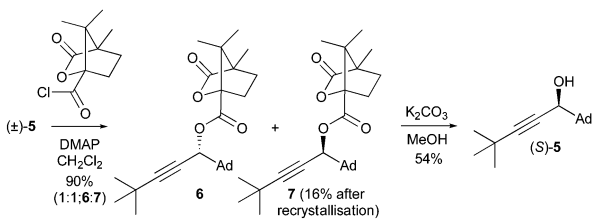

Scheme 2 Resolution of propargylic alcohol (±)-**5** *via* fractional crystallisation of camphanic esters **6** and **7** and subsequent hydrolysis.

 This journal is © The Royal Society of Chemistry 2022

Open Access Article. Published on 24 March 2022. Downloaded on 12/4/2025 8:37:25 AM.
This article is licensed under a Creative Commons Attribution 3.0 Unported Licence.

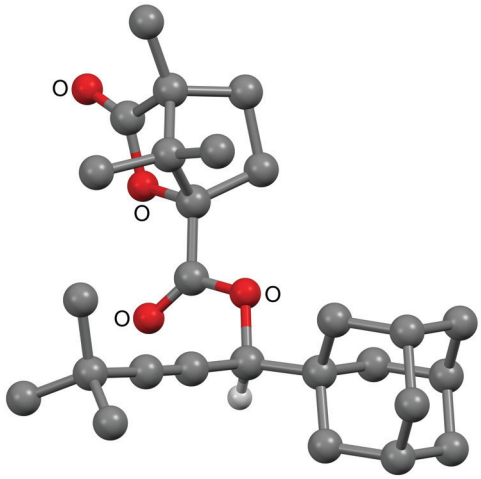

Fig. 4 X-Ray crystal structure of ester **7**.

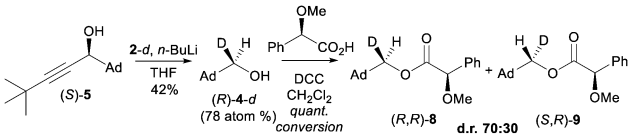

Scheme 3 Hydride transfer from single enantiomer (*S*)-**5** to labelled aldehyde **2**-*d* and derivatisation as (*R*)-*O*-mandelate esters **8** and **9**.

(*S*)-**4**-*d* (+0.21, *c* 2.33 in cyclopentane, e.e. 34 ± 5).[10] This assignment as enriched in (*R*)-enantiomer of **4**-*d* was also supported by measurement of the VCD spectrum and comparison with DFT calculations (B3LYP + GD3BJ/Def2-QZVPP/SCRF = CCl_4)[11] and also by (*R*)-*O*-methylmandelate derivatisation of alcohol **4**, which showed a *ca.* 2 : 1 ratio of diastereomeric esters (*R*,*R*)-**8** and (*S*,*R*)-**9** for which the major isomer can also be assigned as (*R*,*R*)-**8** on the basis of a previous assignment (Fig. 5 and 6).‡‡[12]

The experimental observation of the (*R*)-**4**-*d* enantiomer configuration as the major isomer formed in this experiment is therefore consistent with transition state model **TS B** (Fig. 1). In turn, this is in agreement with our computations which

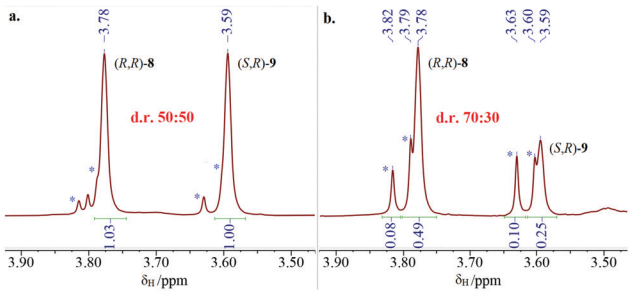

Fig. 5 ^{1}H NMR spectra of diastereomeric mandelate esters (*R*,*R*)-**8** and (*S*,*R*)-**9** showing the resolved $AdCHDO_2CCH(OMe)Ph$ protons in the 3.50–3.90 ppm region from (a, left) (±)-alcohol **4** and (b, right) hydride transfer derived alcohol **4**. The additional peaks in the spectra (*) are diastereotopic methylene protons of $AdCH_2O_2CCH(OMe)Ph$.

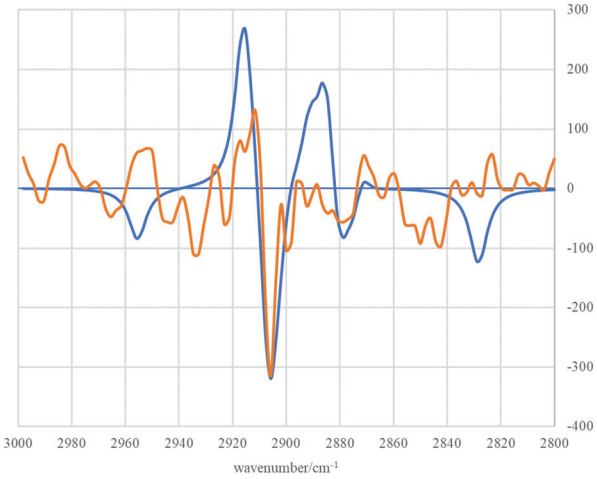

Fig. 6 Experimental (orange line) and calculated (blue line) VCD spectra of (*R*)-**4**-*d* in the region 3000–2800 cm^{-1}.

predicted stabilising contributions from attractive dispersion forces operating between the ^{t}Bu-alkynyl and adamantyl groups. That such attractive dispersion forces can play a role in controlling transition state assemblies and thence stereochemical outcome is notable and may be more widespread than is currently appreciated.[13,14]

NL, KO and HSR performed the calculations, KO and DO performed the synthetic procedures, DCB and HSR wrote the text and all authors edited to the final version.

We thank the Royal Society of Chemistry for a Undergraduate Research Bursary (to K. O.) and the EPSRC for a studentship (to D. O'R.).

Conflicts of interest

There are no conflicts of interest to declare.

Notes and references

‡ We also considered and computed transitions states **C** and **D** (below) with the alkynyl substituent in the equatorial position by inverting the configuration of the alkoxide stereocentre from (*S*) to (*R*). Minimisation of these transition state geometries resulted in their convergence to **TS B** and **A** respectively with identical energies but now with (*R*,*Re*) and (*R*,*Si*) descriptors (*i.e.*, as their enantiomeric forms). These calculations therefore reveal that there are only two diastereomeric transition states for the system regardless of whether the alkyne or adamantyl substituents are initially designated axial or equatorial.

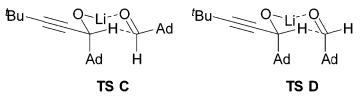

§ Atom % D for deuterated compounds were assessed by quantitative NMR methods integrating relevant signals in ^{1}H NMR and/or inverse-gated ^{13}C spectra. See ESI† for details.

¶ A secondary kinetic isotope effect is evident here in the low isolated yield and reduced atom % D of product **5**-*d*.

‖ We invoke nucleophilic *O*-attack of the lithium alkoxide of (±)-**5**-*d* on AdCHO followed by hydride transfer from the so-formed tetrahedral intermediate to another AdCHO molecule to initiate this process, but the expected adamantanoate ester product could not be identified in

Open Access Article. Published on 24 March 2022. Downloaded on 12/4/2025 8:37:25 AM.
This article is licensed under a Creative Commons Attribution 3.0 Unported Licence.

the product mixture. In support of a Tischenko-type process ester $AdC(O)OCH_2Ad$ could be identified as another component in the mixture as confirmed by comparison with an authentic sample.

** See ESI† for details.

†† Benzoylation of the recovered unreacted alcohol **5** after chromatography and HPLC analysis on a chiral stationary phase and comparison with an authentic racemic sample showed that it was single enantiomer, thus ruling out a reversible reaction for the hydride transfer.

‡‡ A secondary kinetic isotope effect is again in evidence here in the reduced atom % D of product **4**-*d*. This subsequently results in the observation of diastereomeric methylene protons of $AdC\underline{H}_2O_2CCH(OMe)Ph$ in the ^{1}H NMR spectrum of **8** and **9** as a pair of doublets integrating for approximately 24% of the mixture (*cf.*, 22% $AdC\underline{H}_2OH$ in **4**-*d*).

1 D. C. Braddock, A. Mahtey, H. S. Rzepa and A. J. P. White, *Chem. Commun.*, 2016, **52**, 11219–11222.
2 For an early example involving the reduction of hexamethyl acetone to di-*tert*-butyl carbinol with ^{t}BuLi see: P. D. Bartlett, C. G. Swain and R. B. Woodward, *J. Am. Chem. Soc.*, 1941, **63**, 3229–3230.
3 For reductions with lithium dialkylamines see: M. Majewski and D. M. Gleave, *J. Organomet. Chem.*, 1994, **470**, 1–16.
4 For hydride transfer from lithium alkoxides to perfluoroalkyl ketones see: (*a*) Y. S. Sokeirik, K. Sato, M. Omote, A. Ando and I. Kumadaki, *J. Fluorine Chem.*, 2006, **127**, 150–152; (*b*) Y. S. Sokeirik, K. Sato, M. Omote, A. Ando and I. Kumadaki, *Tetrahedron Lett.*, 2006, **47**, 2821–2824. For hydride transfer from lithium alkoxides to diaryl ketones see: (*c*) E. C. Ashby, A. B. Goel and J. N. Argyropolous, *Tetrahedron Lett.*, 1982, **23**, 2273–2276.
5 For all managed computational and experimental FAIR research data, including input and output files, see: D. C. Braddock, N. Limpaitoon, K. Oliwa, D. O'Reilly, H. S. Rzepa and A. J. P. White, Imperial College Research Data Repository, 2021, DOI: 10.14469/hpc/9237 and sub-collections referenced therein.
6 Free energies, 3D transition state models and NCI (non-covalent-analysis) plots can be found at D. C. Braddock, N. Limpaitoon, K. Oliwa, D. O'Reilly, H. S. Rzepa and A. J. P. White, Imperial College Research Data Repository, DOI: 10.14469/hpc/9869.
7 F. A. Luzzio, R. W. Fitch, W. J. Moore and K. J. Mudd, *Angew. Chem., Int. Ed.*, 1999, **76**, 974–975.
8 This effectively constitutes an example of 'Experiment C' as in this excellent essay: E. M. Simmons and J. F. Hartwig, *Angew. Chem., Int. Ed.*, 2012, **51**, 3066–3072.
9 For an excellent overview of pre-existing methods of deuterated aldehyde synthesis, and for RCDO preparation directly from RCHO, see: H. Geng, X. Chen, J. Gui, Y. Zhang, Z. Shen, P. Qian, J. Chen, S. Zhang and W. Wang, *Nat. Catal.*, 2019, **2**, 1071–1077.
10 C. J. Reich, G. R. Sullivan and H. S. Mosher, *Tetrahedron Lett.*, 1973, **17**, 1505–1508.
11 For measured and computed VCD spectra, see D. C. Braddock, N. Limpaitoon, K. Oliwa, D. O'Reilly, H. S. Rzepa and A. J. P. White, Imperial College Research Data Repository, 2022, DOI: 10.14469/hpc/9239 We thank Jordan Nafie, BioTools Inc, Florida, USA for the measurement (CCl4, 75 000 scans, 72 h).
12 S. H. Liggero, R. Sustmann, P. von and R. Schleyer, *J. Am. Chem. Soc.*, 1969, **91**, 4571–4573.
13 For a report of dispersive stabilisation controlling stereoselectivity see: (*a*) E. H. Krenske, K. N. Houk, A. G. Lohse, J. E. Antoline and R. P. Hsung, *Chem. Sci.*, 2010, **1**, 387–392; (*b*) For a rate acceleration through dispersive interactions see: R. Warmuth, J.-L. Kerdelhué, S. Sánchez Carrera, K. J. Langenwalter and N. Brown, *Angew. Chem., Int. Ed.*, 2002, **41**, 96–99; (*c*) For cooperative weak dispersive interactions actuating catalysis see: Y. Wang, M. Rickhaus, O. Blacque, K. K. Baldridge, M. Juríček and J. S. Siegel, *J. Am. Chem. Soc.*, 2022, **144**, 2679–2684.
14 For a review entitled 'London Dispersion in Molecular Chemistry – Reconsidering Steric Effects' see: J. P. Wagner and P. R. Schreiner, *Angew. Chem., Int. Ed.*, 2015, **54**, 12274–12296.

 This journal is © The Royal Society of Chemistry 2022